Non-invasive respiration monitoring by thermal imaging to detect sleep apnoea

USMAN, Muhammad, EVANS, Ruth, SAATCHI, Reza <http://orcid.org/0000-0002-2266-0187>, KINGSHOTT, Ruth and ELPHICK, Heather

Non-Invasive Respiration Monitoring by Thermal Imaging to Detect Sleep Apnoea

Usman, Muhammad.[1], Evans, Ruth.[1] ✉, Saatchi, Reza.[1], Kingshott, Ruth.[2] and Elphick, Heather.[2]

[1] Materials and Engineering Research Institute, Sheffield Hallam University, Sheffield, U.K.
[2] Sheffield Children's NHS Foundation Trust, Sheffield, U.K.
ruth.evans@shu.ac.uk

Abstract. Accurate airflow measurements are vital to diagnose apnoeas; respiratory pauses occurring during sleep that interrupt airflow to the lungs. Apnoea diagnosis usually requires an overnight polysomnography during which numerous vital signs are monitored, including respiratory rate and airflow. The current gold standard in respiration monitoring is a nasal pressure sensor which is placed inside the nostrils of the patient and through which the airflow is measured. Due to the contact nature of the sensor, it is often refused or removed during polysomnography, especially in the case of paediatric patients. We have found that around 50% of children refuse the use of nasal prongs due to its invasiveness, and of those that accepted it, 64% removed the sensor over the course of the polysomnography. We evaluated a non-contact method to monitor respiration by developing infrared thermal imaging, whereby temperature fluctuations associated with respiration are measured and correlated with airflow.
A study was carried out on a sample of 11 healthy adult volunteers whose respiratory signals were recorded over four simulated apnoea scenarios. The respiratory signal obtained through thermal imaging was compared against the gold standard nasal pressure sensor. In 70% of cases, apnoea related events were well correlated with airflow sensor readings. In 16% of recordings the subject's head position did not allow correct identification of the region of interest (i.e. the nostrils). For the remaining 14% of cases there was partial agreement between the thermal measurements and airflow sensor readings. These results indicate thermal imaging can be valuable as a detection tool for sleep apnoea, particularly in the case of paediatric patients.

Keywords: Thermal Imaging, Sleep-Disordered Breathing, Sleep Apnoea.

1 Introduction

Sleep-disordered breathing (SDB) is a term given to apnoea and hypopnoea events that occur during sleep. SDB leads to repetitive episodes of hypoxaemia and sleep fragmentation [1] that can negatively impact the general health of patients with the condition. Apnoeas are defined as a complete cessation of airflow, and hypopnoeas as a partial cessation of airflow [2]. Apnoeas can be classified as central or obstructive. Central apnoea is caused by a brief loss of communication between the central nervous system and the muscles that control respiration. In the case of obstructive apnoea,

a partial or complete collapse of the upper airway is responsible [3]. An apnoeic event in adults is typically categorised as a ≥90% reduction of airflow for at least 10 seconds, while a hypopnea is defined as a ≥30% reduction of airflow for at least 10 seconds associated with a ≥3-4% oxygen desaturation or arousal from sleep [4].

The diagnosis of SDB relies on an investigation known as polysomnography (PSG) during which the patient is recorded overnight to measure their sleep characteristics. Multiple physiological variables are measured as part of the PSG including electrocardiogram (ECG), electroencephalogram (EEG), electrooculogram (EOG), electromyogram (EMG), leg EMG, blood oxygen saturation level (pulse oximetry), chest and abdominal wall movements, airflow, actimetry, body position, snoring, audio and video recordings. In many cases, a limited cardio-respiratory polygraphy (CRPG) study is undertaken which has fewer sensors attached than the full-PSG. The measurements taken during CRPG include chest and abdominal wall movements, airflow, actimetry, body position, snoring, audio and video recordings.

The contact nature and the proximity of airflow sensors to the nose can be problematic during PSG, particularly for paediatric patients. They may cause discomfort and result in distress, soreness and disturbed sleep [5][6]. The two airflow sensors typically used to monitor respiration are both contact methods; nasal prongs measure respiratory airflow directly through nares of the nose, and oro-nasal thermistors detect changes in air temperature under the nose associated with breathing. The nasal prongs are the sensor of choice to detect hypopnoeas as the airflow is directly measured, and oro-nasal thermistors are the sensor of choice to detect apnoeas (alongside respiratory inductance plethysmography bands, RIPs). A study conducted by the Sheffield Children's Hospital of 100 children who underwent an overnight CRPG showed that just 18% of children wore the nasal prongs and 25% wore the thermistor over the full duration of the study. Without these vital pieces of diagnostic information, it is increasingly difficult to accurately diagnose sleep apnoea or other sleep-disordered breathing. Developments that could lead to unobtrusive and contactless respiratory airflow monitoring can therefore be of importance to improving respiratory event detection.

1.1 Thermal Imaging

Thermal imaging can be used to measure respiration-related skin temperature changes centered under the tip of the nose and nostril regions [7]. Exhalation increases the skin temperature while inhalation reduces the temperature in this region. The remote monitoring of breathing function via infrared thermography has been previously explored and shown to be viable by [6]. They record thermal video of the patient and automatically identify the region of interest (ROI) in the first frame of the recording. The ROI is tracked over subsequent frames to compensate for body movements in which the ROI would change position within the frame. Once the ROI is located and successfully tracked, the average value of pixels contained within the region is calculated for

each frame. For successive frames, the mean value represents the breathing signal plotted against time. A number of other studies have also demonstrated the effectiveness of thermal imaging for measuring respiratory airflow and respiration rate [7][8][9].

Thermal infrared imaging has been used more specifically to detect apnoea and hypopnoea events, using traditional surrogate nasal prongs for comparison against during PSG [10]. They used a network of collaborative particle filter trackers (coalitional tracking) to deal with the dynamics of problematic thermal facial tracking. The thermal airflow signal was obtained using the mean temperature of segmented nostril region, and a continuous wavelet transform was used to separate the respiration signal from unwanted components. In this paper, we explore the effectiveness of thermal imaging as a method to monitor various apnoea scenarios that involve normal breathing, obstructive apnoea, hypopnoea and central apnoea. We simultaneously take measurements via the gold standard nasal prongs and respiratory inductance bands as a comparison against the signal obtained by thermal imaging. Remote recordings of patients require body movements to be accounted for and dealt with to record accurate data from the ROI. Even minute body movements cause the ROI to appear in different locations in successive recorded images and thus a tracking method is needed to locate the ROI in each frame.

In Section 2 we outline a number of commonly-used facial and object tracking algorithms and compare their efficacy for the purposes of remote thermal imaging for respiration monitoring. The methodology is described in Section 3, and results of our study and a discussion of the results are presented in Section 4.

2 Tracking Methods

The inside corners between the eyes are the warmest areas on the human face and have the most stable temperature over time. This region can be seen in Figure 1 where brighter areas represent warmer regions. The inner corners of the eyes have been used as distinctive reference points for locating the respiratory region of interest (ROI) under the tip of the nose [7].

A number of tracking methods have been reported that are developed primarily for optical images, however the methods could also be applied to thermal images. Template matching-based tracking is a relatively simple approach where a template of the object to be tracked is segmented from a section of the first image and a correlation process identifies a section in each successive image with closest recumbence. If the object being tracked is significantly inconsistent from one frame to the next, for example by being partially visible or no longer visible, the method will fail [11]. The template may be updated; however this interrupts the process.

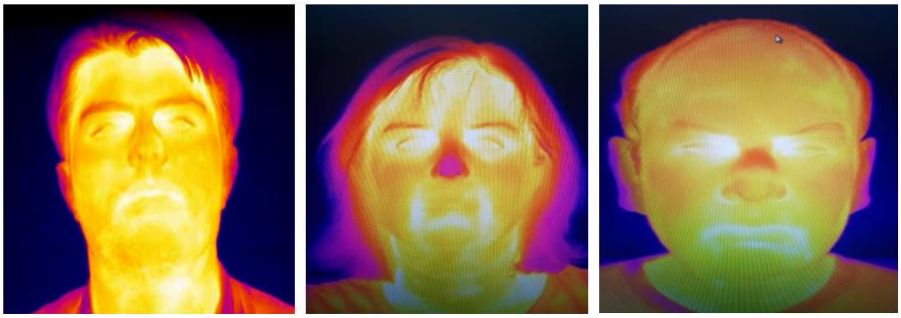

Fig. 1. Thermal images of the faces of adult volunteers.

Coalitional tracking based on partial filter trackers has been used to handle the dynamics of facial temperature changes [10]. Infrared thermography is a continuously evolving process due to its nature of changes in temperature and it is this behaviour that results in a modelling problem to tracking [12].

2.1 Kanade-Lucas-Tomasi Tracking

In addition to the above methods, there are other tracking algorithms based on different approaches such as sparse representation [13] and Kanade-Lucas-Tomasi (KLT) [14]. The KLT feature tracker has been applied in a number of studies because of its efficiency with respect to the points being tracked, and good performance against other tracking methods [15]. The exact locations of features are pre-defined within a ROI and play an important role for the algorithm's operation. Features are defined as points that are dissimilar to their neighbours such as L-corners, T-junctions or a white dot on a black background etc. The KLT algorithm looks for unique feature points in a ROI and then tracks these points in subsequent images [16].

The operation of KLT has three integral components. (1) A feature detector that identifies salient points in each image that have the highest possibility of being selected in subsequent images. Its output is in the form of array of points, and each point is represented by its pixel co-ordinates. (2) A feature tracker whose task is to take the array of points and attempt to identify the exact location of each feature point in subsequent images. Some of the feature points may get lost in the progression of image sequence which could be due to the feature shifting out of camera's field of view or its transformation in such a fashion that the tracker no longer can identify any similarity with the last frame. (3) A feature manager that ensures the feature set being tracked stays above a given threshold. In cases where tracked features are lost in subsequent images (e.g. moving out of the camera's field of view), the feature manager employs the detector to identify new feature points to replace the lost features. The feature manager also ensures that there is an even distribution of feature points across the image to enhance the uniqueness of tracked features [14].

2.2 Histogram-Based Tracking (CAMShift)

Another method used for tracking throughout this study is histogram-based CAMShift (continuously adaptive mean-shift algorithm) tracking. [17] described a histogram of an image as a graphical representation of the total number of pixels in an image at every distinct intensity value found in that image.
CAMShift is generally being used in the field of security surveillance, artificial intelligence, medical diagnosis and military applications [18]. In this work, the CAMShift algorithm used the histogram of the pixel values to identify the tracked object from the image sequence. There were however some issues encountered when using this algorithm:

i. The tracking algorithm was not good enough to track the nose region in subsequent frames of the images.

ii. The location of the ROI changed as the tracking progressed.

iii. In some videos, the tracked area of the ROI was expanded as the tracking process progressed.

The above issues occurred due to the continuous changing behaviour of the histogram of the nose region in the exhalation and inhalation phases. When the subject inhales the black pixels were highly present, whereas on the other hand, during the exhalation phase the black pixels were absent. So due to the changing behaviour of ROI, due to the effect of respiration, the performance of the histogram-based tracker was not good enough to track the ROI effectively.

Because of these issues, KLT was employed to track head movements and to extract the respiration ROI. The region was chosen as an area close to the nostril as it is most affected by respiration through the nose. Exhalation of respiratory air through the nose causes the skin surface temperature in this region to increase and inhalation reduces its temperature. In this study a situation where the person could breathe through their mouth is not considered.

3 Methodology

3.1 Ethics

Ethical approval to carry out the study was obtained from the ethics committee at Sheffield Hallam University (SHU). As per the guidelines of the University and NHS ethics policies, consent forms were prepared for subjects willing to participate in the study. In addition to the consent forms, information sheets were also prepared for volunteers, explaining the basic purpose of the study, why they were asked to take part in the study, how they are going to be monitored, what if they did want to take

part, how their identities were kept anonymous and what happened to the data once they were recorded.

3.2 Participants

11 adult individuals were recruited from SHU's staff and students. Out of these 11 participants, 8 were males and 3 were females. Their age ranged from 24 to 62 years, with an average age of 36 years and 4 months. The participants are considered to be healthy and not currently taking medications, and no creams or other obstructive materials were present on their skin. These recordings were done to test the results of the framework against the gold standard values of nasal airflow sensor, thorax and abdominal (respiratory effort) bands. The results and findings of these tests were used to improve the effectiveness and accuracy of the developed framework in the monitoring of respiration airflow and diagnosing the pauses in breathing mimicked by the participants of the study.

3.3 System Setup

In this study, an FLIR A655sc thermal camera (FLIR Systems UK, West Malling) and its associated FLIR Research Max 4 software were used to collect the thermographic infrared videos. The camera has a spectral range 7.5-14 micron, image resolution (640 x 480 pixels), low noise equivalent temperature difference (a measure of its thermal sensitivity) less than 0.03 K and image capture rate 50 frames per second. The room temperature remained mostly stable with no significant air currents around the subject.

Participants were recorded in four different scenarios representative of apnoea events, with each recording lasting 5 minutes. Two scenarios were associated with normal (quiet) breathing (QB) pattern and the other two scenarios were for irregular breathing (IB) pattern. The four scenarios are outlined below.

QB1: Thoracic and abdominal respiratory inductance plethysmography (RIP) bands were attached to the subject and the instruction was to breathe normally. These detected chest and abdominal wall movements caused by respiration. The device used for this purpose was SOMNOtouchTM RESP (SOMNOmedics Germany) that records thorax and abdomen respiratory effort. The signal sample rate for the device was 32 samples per second. The purpose of this scenario was to investigate the method's ability to measure breathing without any sensor being attached to the face.

QB2: In this scenario, the airflow sensor (nasal prongs) as well as the thoracic and abdominal bands were attached to the subject. The subject breathed normally. The signal sample rate for the airflow sensor was 256 samples per seconds. The purpose of this scenario was to investigate the method's ability to measure respiratory airflow prongs placed in the nares of the nose.

IB1 The thoracic and abdominal bands were attached to the subject. the subject was guided to go through a breathing sequence that consisted of: 1 minute normal breathing, about 10 seconds pause in breathing and no chest or abdominal movement (representing central apnoea), 30 seconds normal breathing, 10 seconds pause in breathing at the nose and mouth with chest and abdominal movement (representing obstructive apnoea), 30 seconds normal breathing, reduction in airflow in breathing at the nose and mouth with continued chest and abdominal breathing (representing hypopnoea) and the remaining recording period normal breathing. The purpose of this scenario was to investigate the method's ability to detect various types of apnoea and hypopnoea without any sensor attached to the face.

IB2: In this scenario the recording pattern was the same as IB1 but other than the thoracic and abdominal sensors the airflow was measured by placing the nasal prongs in the nares of the nose. The purpose of this scenario was to investigate the method's ability to detect various types of apnoea and hypopnoea with the airflow sensor attached to the face. The presence of the nasal airflow sensor was necessary as it is the current gold standard for detecting hypopnoeas but comparison of the findings from IB1 and IB2 would indicate how this sensor affected the thermal imaging results. Figure 2 shows the series of breathing scenarios that volunteers were asked to complete for both the IB1 and IB2 scenarios.

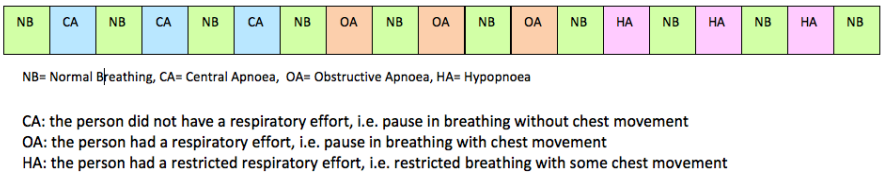

Fig. 1. Series of breathing scenarios that volunteers completed for IB1 and IB2 scenarios.

3.4 ROI Tracking

In this study, KLT makes use of spatial intensity information to direct the search for the position that yields the best match in subsequent frames of a video. It is computationally faster than the traditional practices for observing less potentially correct matches between two images. Figure 3 shows a flow chart explaining the functionality of the KLT algorithm used for this work.

To operate the KLT method, the first recorded image was displayed using Matlab image processing toolbox on a computer screen and a rectangle was manually placed on the nose as shown in the thermal image of Figure 4(a). The ROI was selected to only contain bare skin. The coordinates of the top left corner and bottom right corner of box were used to segment the section and the section was used as template by the KLT method to track the region in the successive images. The nostrils within the selected template provided the best indication of respiratory airflow. This is illustrated

in Figures 4(a) for an image during exhalation and Figure 4(b) for inhalation during respiration.

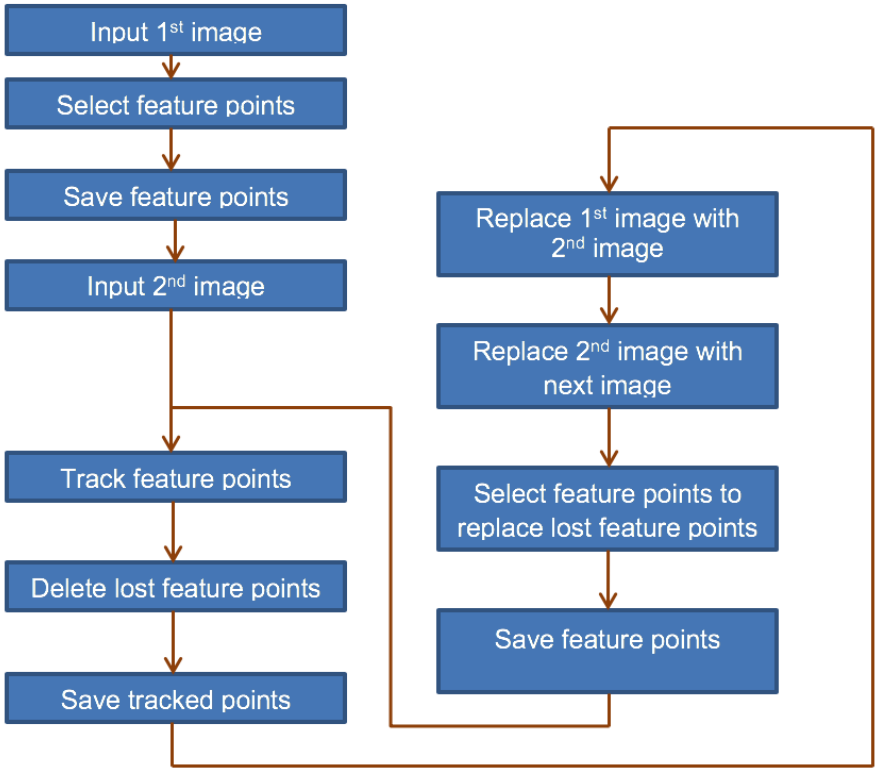

Fig. 3. Flow chart of the functionality of the KLT algorithm.

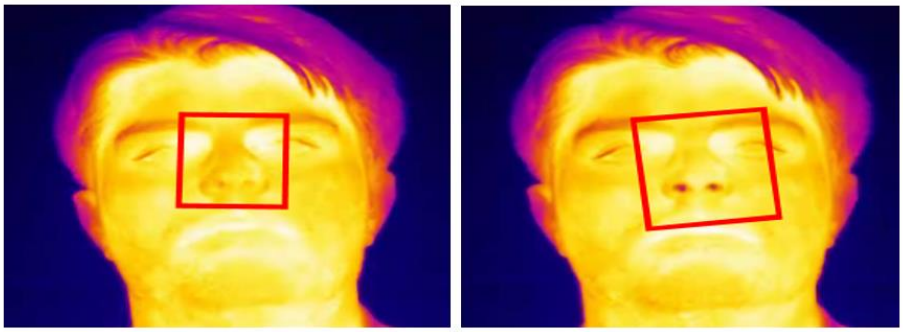

Fig. 4. Thermal images of a participant during the KLT tracking stage. Left: Figure 4(a) shows the initial ROI during exhalation. Right: Figure 4(b) shows a subsequent frame in which the participant is inhaling. The tracked ROI is indicated by the red square.

Application of the KLT tracking algorithm resulted in identification of the facial region containing the nose in each image. The algorithm required a pixel selection threshold with the identified template to be stated. The threshold value varied from person to person as the respiratory airflow volume in individuals was different. Also, the size of the nostrils affected the threshold value. In this study the threshold was provided by experimenting with different values and using the one that provided clearest respiratory signal. The selected pixels were then counted by the algorithm in the successive images and a plot of their count against time provided the thermal imaging based respiratory signal, or thermflow. Figure 5 illustrates the effect of nasal prongs on KLT operation which were used as a comparison in breathing scenarios QB2 and IB2.

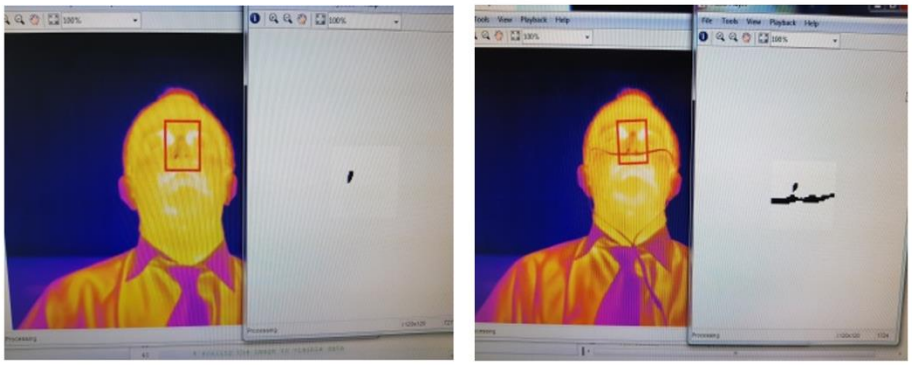

Fig. 5. The effect of nasal prongs on detecting the ROI (a) left: without nasal prongs and (b) right: with nasal prongs.

The presence of nasal prongs in the images has resulted in an increased number of selected pixels (shown as black dots on the right-hand side of each image) at the nostrils. The nasal prongs are made from plastic that is connected to a tube into the electronic device that receives the respiratory airflow signal and quantifies it. As the air passes through the prongs and its associated tube, it increases its temperature during exhalation. Therefore, with the nasal prong attached the area affected by respiratory process increases causing a larger number of pixels to be being counted. The ultimate aim of this study is to exclude the nasal prongs but its presence in this study is needed to act as a valid reference.

The thermflow (respiratory signal) obtained using thermal imaging was analysed against the standard results for nasal airflow, thoracic and abdominal RIP bands and the RIP sum channel. The sum channel is used to identify paradoxical breathing, as it is possible that wall chest and abdomen can move out of synch with one another. The respiratory events can then be broadly classified as central, obstructive or hypopnoeic in pattern using the airflow signal from nasal prongs and RIP sum, and the thermal imaging signal and the RIP sum.

4 Results and Discussion

Tables 1 and 2 indicate the performance of the thermal imaging method to detect central apnoeas, obstructive apnoeas and hypopnoeas. The sleep physiologist considered an event correctly detected or not detected depending upon the scoring rules as described in Section 1 for obstructive, central and hypopnoeas.

Table 1. IB1 Results when nostril was chosen as ROI (no airflow sensor).

Apnoea Type	Correctly Detected	%Correct Detection
Central	7	63.6
Obstructive	7	63.6
Hypopnoea	6	54.0

Table 2. IB1 Results when nostril was chosen as ROI (with airflow sensor).

Apnoea Type	Correctly Detected	%Correct Detection
Central	11	100.0
Obstructive	11	100.0
Hypopnoea	10	91.0

In IB1 where only abdominal and thoracic RIP bands were in place as comparison measures, the percentage correspondence for central, obstructive and hypopnoea were 63.6%, 63% and 54.0% respectively. However, the corresponding results for IB2, where the nasal prongs were in place, were 100%, 100% and 91.0%. The differences in the IB1 and IB2 results are partly due to a better reference for IB2 allowing improved scoring of the results. Another contributing factor is the presence of nasal prongs and the manner it may have influenced the thermal pattern at the site of the measurement. The nasal prongs partially obscured the nostril area thus reducing the thermal visibility of the region being monitored. On the other hand, the prongs and the two tubes directly connected to it transfer respiratory heat making a wider region that is affected by respiration visible to the thermal imaging.

In the following sections a review of the respiratory signals from one subject is carried out as an illustrative example. Figure 6 shows the starting pause in the respiration signal from the airflow nasal pressure sensor (upper) and a similar pause is also present in the respiration signal obtained from the thermal imaging method (lower). Then

there are three pauses representing central apnoea, three pauses representing obstructive apnoeas and finally three pauses representing hypopnoeas. The thermal imaging method successfully detected all the apnoea types mimicked by the subject.

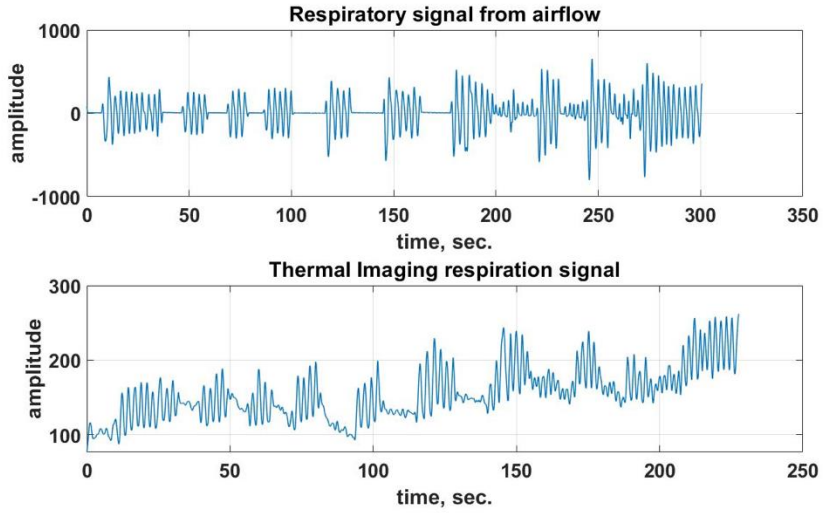

Fig. 6. Respiratory signal from airflow (upper) and respiratory signal from thermal imaging via the KLT ROI tracking algorithm (lower).

4.1 Limitations of the Study

The results obtained by this work show that thermal imaging has the potential to be a powerful diagnostic tool for classifying apnoea and sleep-disordered breathing. There are, however, some limitations to the technology and setup currently available.

This work studied heathy adult volunteers who did not make large body movements; however the technology would be particularly beneficial for paediatric patients who refuse to wear the nasal prongs. In actual clinical practice during overnight sleep recording, a child is likely to make large head and body movements, hence if the camera position is fixed, the child's face may not remain within the camera's field of view and resulting in failure of the method. Therefore, further developments will be needed to take the approach to routine clinical use, particularly for paediatric respiration monitoring.

The adults studied in this work were awake and mimicking respiratory events rather than asleep. True cases of sleep-disordered breathing and apnoea may not be as well defined as was measured for this study.

Another consideration for future studies in this area would be to include thermistor measurements as well as nasal prongs and RIP chest bands. American Academy of Sleep Medicine rules [4] state that the sensor of choice to detect central/obstructive apnoea is the thermistor, however we measured with nasal prongs only (sensor of choice for detecting hypopnoeas). To accurately score the respiratory events, both the airflow channel (nasal prongs/thermistor) and RIP channels are needed as per the scoring rules, however in one of the conditions the nasal prongs were removed hence respiratory events could not be clinically scored in that scenario.

5 Conclusion

The use of thermal imaging for measuring respiratory airflow can be a valuable tool for detecting apnoeas and hypopnoeas and can make the diagnosis process more child-friendly due to its non-contact nature. Tracking plays an important role in identifying the respiratory region of interest in the successive images. In this study a KLT-based tracking algorithm was used and proved effective in its operation. However, the subjects included in this study did not make large body movement and so more developments are needed to cater for applying the methods to recordings in both clinical and the intended paediatric environments.

References

1. T. Young, L. Finn, P. E. Peppard et al., "Sleep Disordered Breathing and Mortality: Eighteen-Year Follow-up of the Wisconsin Sleep Cohort", Sleep, Volume 31, Issue 8, August 2008, Pages 10711078.
2. Kapur, Vishesh K., et al. "Clinical practice guideline for diagnostic testing for adult obstructive sleep apnea: an American Academy of Sleep Medicine clinical practice guideline." Journal of Clinical Sleep Medicine 13.03 (2017): 479-504.
3. Association of Sleep Disorders Centers: Diagnostic Classi_cation of Sleep and Arousal Disorders. Prepared by the Sleep Disorders Classi_cation Committee, Ro_warg HP. Sleep 1979;2:1-137.
4. International Classi_cation of Sleep Disorders: Diagnostic and Coding Manual. 2. Westchester: American Academy of Sleep Medicine; 2005.
5. L. Chen, X. Zhang and C. Song, An Automatic Screening Approach for Obstructive Sleep Apnea Diagnosis Based on Single-Lead Electrocardiogram, IEEE Transactions on Automation Science and Engineering, vol. 12, no. 1, pp. 106-115, 2015.
6. C. B. Pereira, X. Yu, M. Czaplik, R. Rossaint, V. Blazek and S. Leonhardt, Remote monitoring of breathing dynamics using infrared thermography, Biomedical Optics Express, vol. 6, no. 11, pp. 4378-4394, 2015.
12 Usman, M.ı et al.
7. A. H. Alkali, R. Saatchi, H. Elphick and D. Burke, Thermal image processing for real-time., IET Circuits Devices Systems., vol. 11, no. 2, pp. 142-148, 2017.
8. J. Fei and I. Pavlidis, Thermistor at a distance: unobtrusive measurement of breathing, IEEE Transactions on Biomedical Engineering, vol. 57, no. 4, pp. 988-998, 2009.
9. A. K. Abbas, K. Heimann, K. Jergus, O. Thorsten and S. Leonhardt, Neonatal non-contact respiratory monitoring based on real-time infrared thermaography, Biomedical Enginnering Online, vol. 10, no. 93, pp. 1-17, 2011.
10. J. N. Murthy, J. V. Jaarsveld, J. Fie, I. Pavlidis, R. I. Harrykissoon, J. F. Lucke, S. Faiz

and R. J. Castriotta, Thermal Infrared Imaging: A Novel Method to Monitor Airow During Polysomnography., SLEEP, vol. 32, no. 11, pp. 1521-1527, 2009.
11. X. Mei and H. Ling, Robust Visual Tracking and Vehicle Classi_cation via Sparse Representation, IEEE Transactions on Pattern Analysis and Machine Learning, vol. 33, no. 11, pp. 2259-2272, 2011.
12. J. Fei, I. Pavlidis and J. Murthy, Thermal Vision for Sleep Apnoea Monitoring, in Springer-Verlag, Berlin Heidelberg, 2009.
13. Y. Cho, S. J. Julier, N. Marquardt and N. Bianchi-Berthouze, Robust Tracking of Respiratory Rate in High-Dynamic Range Scenes Using Mobile Thermal Imaging, Biomedical Optical Express, vol. 8, no. 10, pp. 1-24, 2017.
14. B. Barnes , D. Abeywardena, S. Kodagoda and G. Dussanayake, Evaluation of Feature Detectors for KLT based Feature Tracking using the Odroid U3, in Proceedings of Australian Conference on Robotics and Automation., Melbourne, 2014.
15. H. Fassold, P. Schallauer, J. Rosner and W. Bailer, Realtime KLT Feature Point Tracking for High De_nition Video, ResearchGate, 2009.
16. Z. Zivkovic and F. v. d. Heijden, Improving the selection of feature points for tracking, Pattern Analysis and Applications, vol. 7, no. 2, pp. 1-17, 2004.
17. R. C. Gonzalez and R. E. Woods, Digital Image Processing., New Jersey.: Prentice Hall., 2007.
18. Y. Cho, S. J. Julier, N. Marquardt and N. Bianchi-Berthouze, "Robust Tracking of Respiratory Rate in High-Dynamic Range Scenes Using Mobile Thermal Imaging," Biomedical Optical Express, vol. 8, no. 10, pp. 1-24, 2017.